J. Min. Metall. Sect. B-Metall. 48 (2) B (2012) 319 - 324

Journal of Mining and Metallurgy

THE PRECIPITATION OF NANOCRYSTALLINE STRUCTURE IN THE JOULE HEATED $Fe_{72}Al_5Ga_2P_{11}C_6B_4$ METALLIC GLASSES

N. Mitrović[*,#], S. Kane[**], S. Roth[***], A. Kalezić-Glišović[*], C. Mickel[***], J. Eckert[***]

[*]Joint Laboratory for Advanced Materials of SASA, Section for Amorphous Materials, University of Kragujevac, Technical Faculty Čačak, Svetog Save 65, 32 000 Čačak, Serbia,
[**]School of Physics, D. A. University, Indore-452017, India,
[***]Leibniz Institute for Metallic Materials, IFW Dresden, P.O.Box 270016, D-01171 Dresden, Germany

(Received 19 July 2011; accepted 01 October 2011)

Abstract

In this study, the evolution of the nanostructure on dc Joule heated $Fe_{72}Al_5Ga_2P_{11}C_6B_4$ metallic glass ribbons have been investigated. Heating power per square area (P_S) was ranging between 0.8 to 7.1 W/cm^2 in order to get various stages of relaxation or nanocrystallization. The crystallization starts after applying $P_S \approx$ 4.35 W/cm^2 and the sample consist of residual amorphous matrix, a magnetic crystalline component and also a non-magnetic crystalline component (relative abundance of Fe in the crystalline phase is about 35 %). XRD measurements show that crystalline samples after current annealing consist of Fe_3B, FeC, FeP and Fe_3P compounds. On TEM micrograph a broad distribution of shapes and sizes is noticed, the latter range from about 60 to 350 nm, increasing by applied heating power. The decrease of the electrical resistivity after each current annealing treatment is rather small in comparison with other Fe-based amorphous alloys (only about 1.5 % for the highest P_S). Partial nanocrystallization leads to increase of coercive field (from $H_C \approx$ 7 A/m in the amorphous as-cast state up to 45 A/m) attributed to precipitation of magnetically harder compounds (Fe_3B and FeC).

Key words: *Metallic glasses, Thermal properties, Nanocrystallization, Transmission electron microscopy, Mössbauer spectra, Electrical measurements, Magnetic measurements.*

[#] *Corresponding author: nmitrov@tfc.kg.ac.rs*

DOI:10.2298/JMMB110719018M

1. Introduction

The development of the iron based bulk metallic glasses in the nineties has attracted a large interest due to established rules for the stabilization of supercooled liquid as well as due to possibility for technical application [1]. Moreover, alloys of Fe-(Al, Ga)-(P, C, B, Si) system are among the softest Fe-based amorphous and nanocrystalline magnetic materials [2]. The amorphous state of matter is structurally and thermodynamically unstable and very susceptible to partial or complete crystallization [3] during thermal treatment. Beside the benefits of energy and time saving due to relative short time treatment [4], Joule heating brings development of specific structural transformations [5] that could not be attained by conventional (furnace) annealing. Nowadays, there are a variety of methods to apply this technique: (a) single treatment with different current intensities and pulse duration [6]; (b) multi-step treatments with successive increase in current intensity with [7] or without cooling [8] between the steps; (c) application of high frequency currents [9]. In this paper we report the precipitation of the nanocrystalline structure on dc Joule heated $Fe_{72}Al_5Ga_2P_{11}C_6B_4$ metallic glass ribbons by multi-step treatments with cooling between the steps.

2. Experimental

Ribbons of nominal composition $Fe_{72}Al_5Ga_2P_{11}C_6B_4$ about 30 nm thick and 3.5 mm wide were prepared by single-roller melt-spinning in air. The thermal stability was examined by differential scanning calorimetry (Perkin-Elmer DSC 7). Samples of the ribbons 100 mm long were processed by *dc* Joule heating for 60 s in air and then slow-cooled by ramping down annealing current at rate of 5 mA/s. Heating power per square area (P_S) was ranging between 0.8 to 7.1 W/cm^2 in order to get various stages of relaxation or nanocrystallization. Crystallization behavior were examined by X-ray diffraction (XRD) with a Philips PW 1820 diffractometer ($Co_{K\alpha}$ radiation λ=0.1789 nm) and transmission electron microscopy (TEM JEOL 2000 FX). On-line and post-annealing electrical resistivity measurements were performed by the four point method [7]. In addition, transmission Mössbauer spectra recorded at room temperature using ^{57}Co:Rh source as well as magnetic B-H hysteresis measurements [10, 11] were used for characterization of structural changes evolved during current annealing (CA) treatments.

3. Results and discussion

Figure 1 shows DSC trace for the $Fe_{72}Al_5Ga_2P_{11}C_6B_4$ alloy. The wide supercooled liquid region between crystallization temperature and glass transition temperature ($\Delta T_x = T_x - T_g$ = 65 K) as well as Curie temperature (position of the 'λ-peak': T_C = 574 K) were observed. High value of the reduced glass transition temperature $T_{rg} = T_g/T_l$ of about 0.54 is characteristic of an alloy with good glass forming ability [12] and high thermal stability against crystallization (T_l is liqiudus temperature). The existence of a large ΔT_x region allows annealing above T_g in the supercooled liquid state and efficient stress relief can be attained.

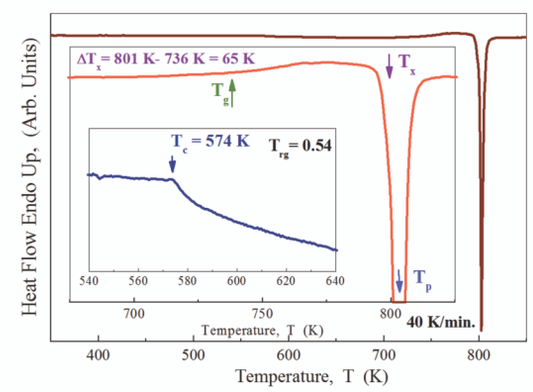

Fig. 1. DSC thermogram of $Fe_{72}Al_5Ga_2P_{11}C_6B_4$ amorphous alloy obtained at heating rate of 40 K/min. The insets show determination of characteristics (onset) temperatures (Tx crystallization temperature, Tg glass transition temperature, T_C Curie temperature).

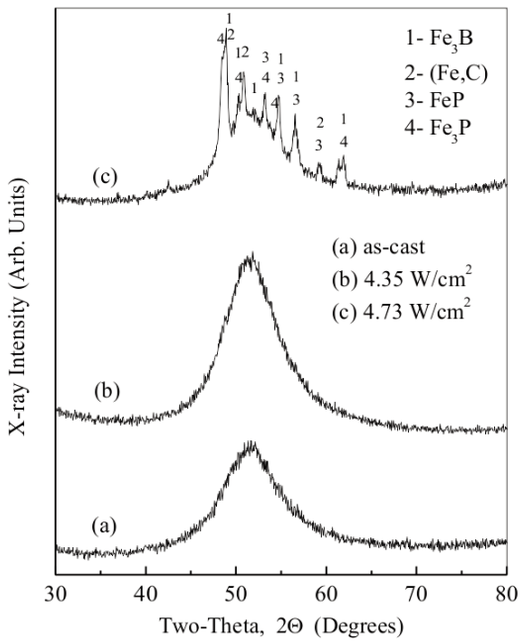

Fig. 2. XRD patterns for the $Fe_{72}Al_5Ga_2P_{11}C_6B_4$ alloy samples in: (a) as-cast state and after CA at (b) 4.35 W/cm^{2}and (c) 4.73 W/cm^2.

In order to get various stages of relaxation or nanocrystallization heating power (P_S) was ranging from very low (0.8 W/cm^2) to very high (7.1 W/cm^2) values. Very early stage of crystallization process was observed after applying $P_S \approx 4.35$ W/cm^2 (Fig. 2b). With increasing heating power, peaks of several iron-metalloid compounds are seen to emerge from the broad diffuse diffraction maximum of an amorphous phase. Therefore, XRD pattern of crystalline sample (Fig. 2c) shows the structure with residual amorphous matrix and iron-metalloid crystalline phase with Fe_3B, FeC, FeP and Fe_3P compounds.

In order to better understand process of crystallization the annealed samples were examined by TEM. Figure 3 shows TEM image and microdiffraction patterns of the CA samples treated by 4.73 W/cm^2 and 5.35 W/cm^2. The average size of the crystallized particles increases with increasing heating power. A broad distribution of shapes and sizes is noticed, the latter range from about 60 to 350 nm. From a big grain, a single crystal diffraction pattern has been observed. The polycrystalline structure is inhomogeneous and very vague and in many cases the grain boundaries are difficult to be seen.

Electrical resistivity of Fe-based metallic glasses is very sensitive to relaxation and crystallization processes [13]. Therefore, we analyze the changes of resistivity vs. applied heating power. As can be seen on Fig. 4 decrease of the normalized sample resistivity after each treatment is rather small in comparison with other Fe-based amorphous alloys [14], only about 1.5 % for the highest P_S.

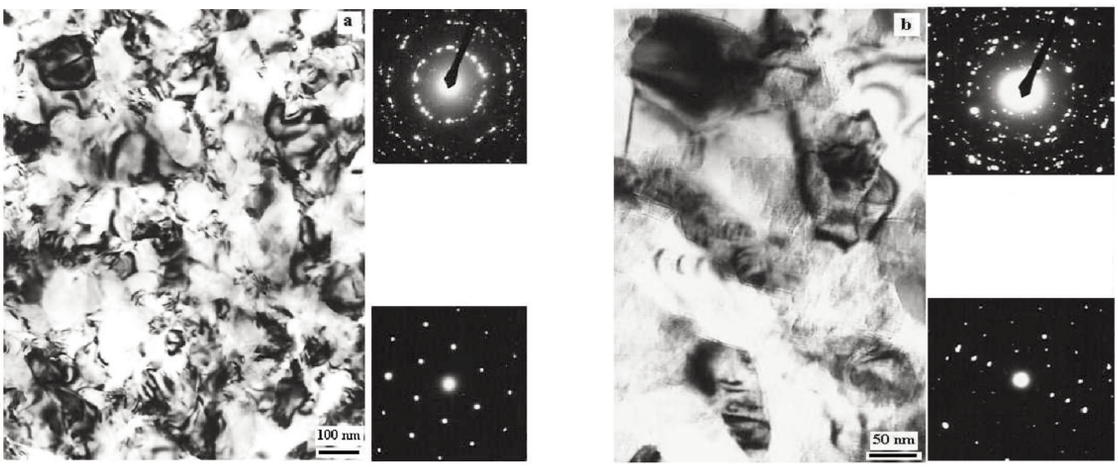

Fig. 3. Bright –field electron micrograph and selected area diffraction patterns of the $Fe_{72}Al_5Ga_2P_{11}C_6B_4$ CA samples treated by (a) 4.73 W/cm^2 and (b) 5.35 W/cm^2.

Mössbauer spectroscopy is applied for microscopic study on the magnetic structure. Figure 5 shows the Mössbauer spectra (experimental data and fit) as well as hyperfine field distribution of the as-cast and crystallized CA samples. There were observed magnetic crystalline component and also a non-magnetic crystalline component (Fig. 5a). It was calculated that the relative abundance of Fe in the crystalline phase is about 35%.

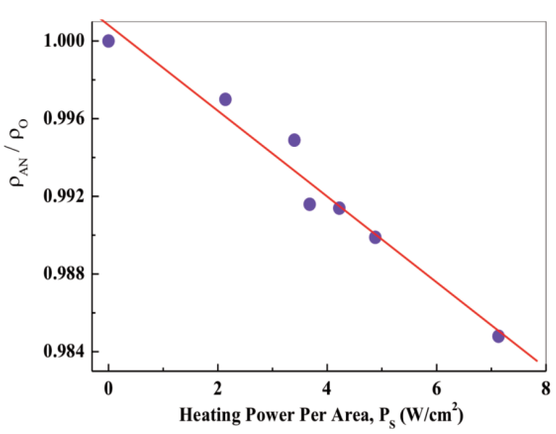

Fig. 4. The changes of resistivity of the $Fe_{72}Al_5Ga_2P_{11}C_6B_4$ annealed samples (ρ_{AN}) normalized to the resistivity in the as-cast state (ρ_O).

Intensity of second and fifth line relative to innermost (third and fourth lines $b=A_{2:5}/A_{3:4}$) is a measure of the spin texture of the sample. In absence of stresses in the specimen, the average atomic spin orientation remains in the ribbon plane due to shape-anisotropy, thus making $b \approx 4$. For a completely random magnetic moments orientation, b is expected to be equal to 2. The value b = 3.24 observed in the as-cast state suggests that spins are preferentially aligned within the ribbon plane due to large in-plane anisotropy. CA treated sample with maximum heating power (P_s=7.1 W/cm^2) have considerable decreased value of b = 2.75 due to changes in the orientation of the net magnetic moment from within the ribbon plane. The decrease in parameter b gives indication for slight transverse anisotropy generated by circular magnetic field obtained via CA. Almost similar values of the fractional width of distribution ΔB_{hf} /<B_{hf}> in as-cast and CA specimen (0.374 and 0.377, respectively) exhibits quite similar values of structural disorder. This can be

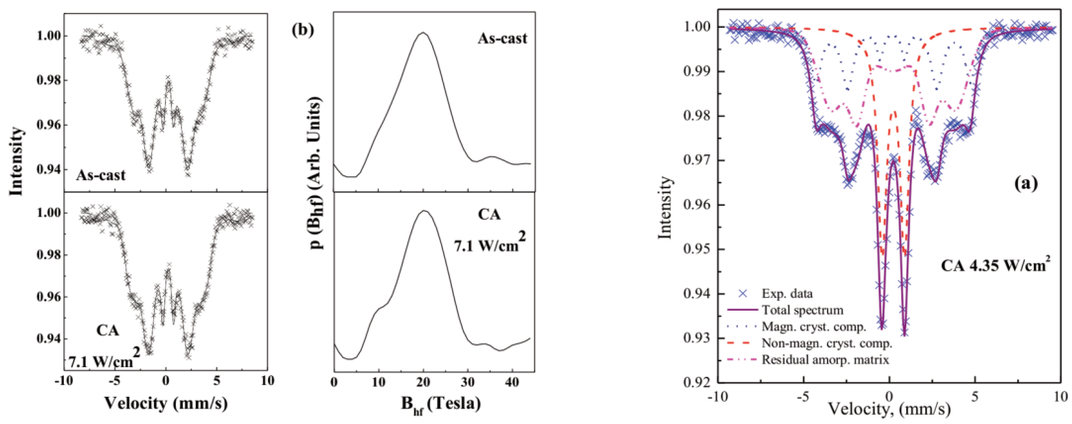

Fig. 5. (a) Mössbauer spectra of $Fe_{72}Al_5Ga_2P_{11}C_6B_4$ CA sample (Ps=4.35 W/cm^2); (b) spectra and corresponding hyperfine field distributions of as-cast and CA (Ps=7.1 W/cm^2) sample.

associated with an already observed slight decrease of electrical resistivity. Hyperfine field distribution on Fig. 5b, apart from the main peak shows a low field hump around 9 T in CA sample that can be attributed to the presence of Ga, P, and C in the first near-neighbors shell of Fe, reducing the Fe magnetic moment [15].

Optimum relaxation of the amorphous structure was approved by coercivity minima of 2 A/m after CA with P_s=3.25 W/cm^2 (Fig. 6a). Hysteresis loops of annealed samples confirm the behaviour of spin texture observed by Mössbauer spectra. It is noticed tilting of loops of CA crystallized samples with significantly reducing remanence due to increase of perpendicular uniaxial anisotropy (Fig. 6b). Further, partial nanocrystallization leads to magnetic hardening, i.e. increase of coercive field attributed to precipitation of magnetically harder compounds (Fe_3B and FeC) was recorded. The nanocrystallites

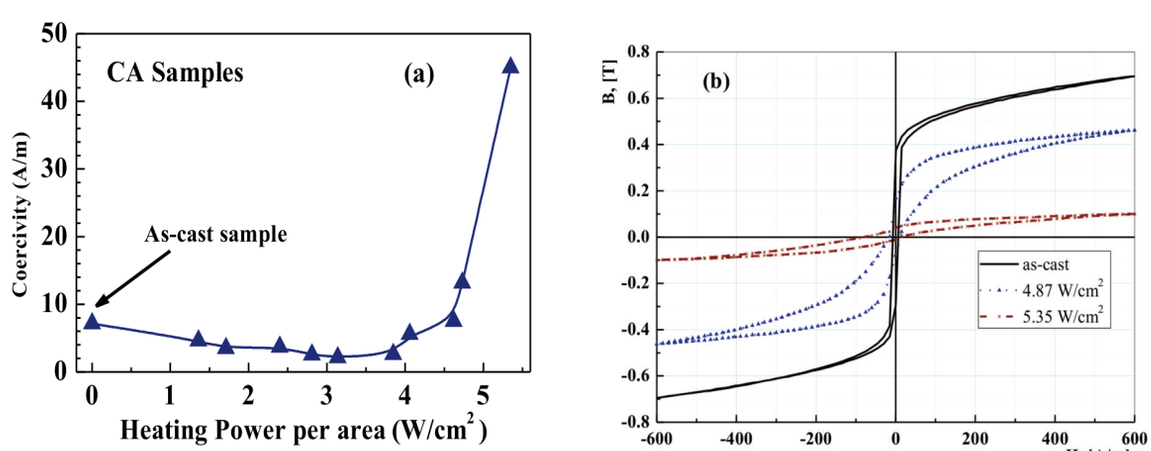

Fig. 6. (a) Coercivity changes of $Fe_{72}Al_5Ga_2P_{11}C_6B_4$ after different CA treatments; (b) comparison of hysteresis loops in as-cast state and after appearance of the nanocrystals in structure.

observed by TEM analysis acts as pinning centers for domain wall movement causing coercivity increase up to 45 A/m.

4. Conclusion

Multistep CA treatments of $Fe_{72}Al_5Ga_2P_{11}C_6B_4$ metallic glass ribbons were used to obtain transformation from amorphous to nanocrystalline structure. Slight transverse anisotropy was generated by circular magnetic field obtained via CA and the presences of Ga, P, and C in the first near-neighbors shell of iron reduce the Fe magnetic moment. Due to a large grain size (more than 60 nm) and precipitation of magnetically hard Fe_3B and FeC compounds it was not attained nanocrystalline structure with improved soft magnetic properties.

Acknowledgements

This work was partially supported by the Serbian Ministry of Science and Technology, Grant No. 172057. The financial support by the German Academic Exchange Service (DAAD) as well as Saxon Ministry for Science and Art is gratefully acknowledged by N. M.

References

[1] T. Bitoh, A. Makino, A. Inoue, Mater. Trans., 44 (2003) 2020.

[2] T. Mizushima, A. Makino, A. Inoue, J. Appl. Phys., 83 (1998) 6329.

[3] E. Illekova, J. Šesták "Crystallization of metallic micro- and nano-crystalline glasses" in the book "Some thermodynamic, structural and behavior aspects of materials accentuating noncrystalline states" (J. Šesták, M. Holeček. J. Málek, edts), OPS-ZČU Plzen, 2009, p. 308.

[4] N. Mitrović, Sci. Sintering, 30 (1998) 85.

[5] N. Mitrović, S. Roth, M. Stoica, J. Alloys Compd., 434-435 (2007) 618.

[6] Z. H. Lai, H. Conrad, G. Q. Teng, Y. S. Chao, Mat. Sci. Eng. A, 287 (2000) 238.

[7] N. S. Mitrović, S. R. Djukić, S. B. Djurić, IEEE Trans. Magn., 36 (2000) 3858.

[8] J. Moya, V. Cremashi, F. C. S. Silva, M. Knobel, H. Sirkin, J. Magn. Magn. Mater., 226-230 (2001) 1522.

[9] H. Lee, Y. K. Kim, K. J. Lee, T. K. Kim, J. Magn. Magn. Mater., 215-216 (2000) 310.

[10] S. Roth, H. Grahl, J. Degmova, N. Schlorke-de Boer, M. Stoica, J. M. Borrego, A. Conde, N. Mitrović, J. Eckert, Journ. Optoel. Advan. Mater., 4 (2002) 199.

[11] S. Djukić, V. Maričić, A. Kalezić-Glišović, L. Ribić-Zelenović, S. Randjić, N. Mitrović, N. Obradović, Sci. Sintering, 43 (2011) 175.

[12] J. Šesták, A. Kozmidis-Petrović, Ž. Živković, J. Min. Metall. Sec. B – Metall. 47 (2) B (2011) 229.

[13] M. Kuzminski, A. S. Waniewska, H. K. Lachowitcz, G. Herzer, IEEE Trans. Magn., 30 (1994) 533.

[14] A. Kalezić-Glišović, L. Novaković, A. Maričić, D. Minić, N. Mitrović, Mat. Sci. Eng. B, 131 (2006) 45.

[15] A. Gupta, S. N. Kane, N. Bhagat, T. Kulik, J. Magn. Magn. Mater., 254-255 (2003) 492.